

Evaluation of a Switched Combining Based Distributed Antenna System (DAS) for Pedestrian-to-Vehicle Communications

Yoo, S., Cotton, S., Zhang, L., Doone, M., Song, J. S. & Rajbhandari, S.

Published PDF deposited in Coventry University's Repository

Original citation:

Yoo, S, Cotton, S, Zhang, L, Doone, M, Song, JS & Rajbhandari, S 2021, 'Evaluation of a Switched Combining Based Distributed Antenna System (DAS) for Pedestrian-to-Vehicle Communications', IEEE Transactions on Vehicular Technology, vol. 70, no. 10, pp. 11005 - 11010.

<https://dx.doi.org/10.1109/TVT.2021.3102700>

DOI 10.1109/TVT.2021.3102700

ISSN 0018-9545

ESSN 1939-9359

Publisher: IEEE

This work is licensed under a Creative Commons Attribution 4.0 License. For more information, see <https://creativecommons.org/licenses/by/4.0/>

Evaluation of a Switched Combining Based Distributed Antenna System (DAS) for Pedestrian-to-Vehicle Communications

Seong Ki Yoo ¹, *Member, IEEE*,
 Simon L. Cotton ², *Senior Member, IEEE*,
 Lei Zhang ³, *Student Member, IEEE*,
 Michael G. Doone ⁴, *Student Member, IEEE*,
 Jae Seung Song ⁵, *Senior Member, IEEE*,
 and Sujan Rajbhandari ⁶, *Senior Member, IEEE*

Abstract—The safety of vulnerable road users is paramount, particularly as we move towards the widespread adoption of autonomous and self-driving vehicles. In this study, we investigate the use of a six-element distributed antenna system (DAS), operating at 5.8 GHz and mounted on the exterior (i.e., roof and wing mirrors) of an automobile, to enhance signal reliability for pedestrian-to-vehicle (P2V) communications. Due to its low complexity and ease of implementation, we consider the use of a switch-and-examine combining with post-examining selection (SECps) scheme to combine the signal received by the DAS. During our experiments, a pedestrian wearing a wireless device on their chest either stood stationary or walked by the side of a road. It was found that the overall signal reliability depends on not only the number, but also different groupings of the antennas which are selected. The goodness-of-fit results have shown that the temporal behavior of the diversity gain was adequately described by the Gaussian distribution. Building upon this, we also provide some useful insights into the antenna selection through the comparison of three different antenna selection mechanisms, namely per-sample random antenna selection, one-shot antenna selection and per-sample optimal antenna selection.

Index Terms—Antenna selection, distributed antenna system, diversity gain, pedestrian-to-vehicle communications, switched combining.

I. INTRODUCTION

Pedestrian-to-Vehicle (P2V) communications and also the reciprocal vehicle-to-pedestrian (V2P) communications are an important part of the so-called vehicle-to-everything (V2X) communications. These occur when a wireless device(s) situated on a person communicates with wireless devices located on a vehicle [1]. They have gained much attention recently as they will enable direct communications between vehicles and vulnerable road users (VRUs) including pedestrians and

Manuscript received November 9, 2020; revised May 21, 2021; accepted July 20, 2021. Date of publication August 5, 2021; date of current version October 15, 2021. This work was supported by the Institute of Information and Communications Technology Planning & Evaluation (IITP) funded by the Korea government (MSIT) under Grant 2021-0-00188. The review of this article was coordinated by Prof. A. J Al-Dweik. (*Corresponding author: Seong Ki Yoo.*)

Seong Ki Yoo is with the Research Centre for Computational Science & Mathematical Modelling, Faculty of Engineering, Environment and Computing, Coventry University, Coventry CV1 2TL, U.K. (e-mail: ad3869@coventry.ac.uk).

Simon L. Cotton, Lei Zhang, and Michael G. Doone are with the Centre for Wireless Innovation, ECIT Institute, Queen's University Belfast, Belfast BT3 9DT, U.K. (e-mail: simon.cotton@qub.ac.uk; lzhang27@qub.ac.uk; mdoone03@qub.ac.uk).

Jae Seung Song is with the Software Engineering and Security Laboratory, Department of Computer & Information Security and Convergence Engineering for Intelligent Drone, Sejong University, Seoul 05006, South Korea (e-mail: jssong@sejong.ac.kr).

Sujan Rajbhandari is with the School of Computer Science and Electronic Engineering, Bangor University, Bangor LL57 1UT, U.K. (e-mail: sujan@ieee.org).

Digital Object Identifier 10.1109/TVT.2021.3102700

cyclists. For example, P2V and V2P communications have been used as the basis for a collision avoidance system [2] and a pedestrian protection system [3]. Additionally, they may act as relay nodes for one another and thus provide multi-hop communications in case of wireless devices existing outside their communication range [4].

In P2V communications, wireless devices are operated in close proximity to the pedestrian's body and vehicle's body while they are mobile. In this case, the direct signal path, i.e., line-of-sight (LOS), between the pedestrian and vehicle is generally obstructed by pedestrian's body and/or vehicle's structure. Due to these shadowing effects, an LOS link between the pedestrian and vehicle is not always available. Under non-LOS (NLOS) conditions, it is well-known that deep fades can occur in the received signal power, which have the potential to reduce the overall signal reliability and the performance of P2V communication systems. One approach, often employed to overcome signal degradation caused by propagation related effects, is the use of a distributed antenna system (DAS) [5]. As in [6], the use of spatially separated antennas in vehicular networks provides many advantages such as a higher packet reception rate and an improvement in the overall received signal strength (RSS).

Switched combining and gain combining schemes are the most widely utilized in conjunction with spatial diversity systems [7] such as DAS. In switched combining schemes, the DAS selects one of the available antennas according to a corresponding criterion. Among the most popular switched combining schemes are pure selection combining (PSC), switch-and-stay combining (SSC), switch-and-examine combining (SEC) and SEC with post-examining selection (SECps). On the contrary, in gain combining schemes, the output of the DAS is formed as a linear combination of the signals received by all of the available antennas. Notable combining techniques here include equal gain combining (EGC) and maximum ratio combining (MRC) schemes.

Over the last few decades, a number of studies have been conducted which investigate the characteristics of V2X communication channels (including P2V communication channels) with the aim of developing V2X based wireless systems [8]–[13]. Also, to this end, a number of antenna diversity techniques have been studied with the aim of increasing signal reliability in the context of vehicle-to-vehicle (V2V) and vehicle-to-infrastructure (V2I) communications [14]–[20]. In contrast, there are comparatively few results on the use of spatial diversity techniques in the context of P2V communications presented in the open literature [18], [21]. Therefore, in this paper, we examine the potential to improve signal reliability for P2V communications at 5.8 GHz¹ when using a switched combining based DAS mounted on the exterior of an automobile. It is widely known that, among the aforementioned switched combining schemes, the SECps scheme provides almost the same performance (with less complexity) as the PSC scheme when the optimum switching threshold is chosen [23]–[25]. Therefore, in this paper, we consider the use of an L -antenna SECps based DAS (where L denotes the number of antennas) and evaluate the corresponding localized diversity gain. We then examine how the selection of different groupings of antennas influences the diversity gain when using three different antenna selection schemes, namely per-sample random

¹This frequency is chosen due to its close proximity to the 5.9 GHz dedicated short-range communications (DSRC) standards in the United State (US) and intelligent transport system-5G (ITS-5G) standards in the European Union (EU), which is designed to support a variety of applications of vehicular network communications [22].

antenna selection [26], one-shot antenna selection [27] and per-sample optimal antenna selection [27].

The remainder of this paper is organized as follows: Section II describes the measurement system, environment and movement scenarios. In Section III, the achievable diversity gain is presented for different numbers of antennas and different groupings of antennas while Section IV presents three different antenna selection schemes along with their performance when used within a P2V based DAS. Finally, Section V concludes the paper with some closing remarks.

II. P2V CHANNEL MEASUREMENTS

A. Measurement System

The measurement system used in this paper consisted of seven bespoke wireless nodes operating at 5.8 GHz. Each node was capable of functioning as either a transmitter (TX) or receiver (RX). For the purpose of the P2V channel measurements, one was configured as a TX and the remaining six as RXs. The TX featured an ML5805, single-chip fully integrated frequency shift keyed (FSK) transceiver,² manufactured by RFMD. This was configured to transmit a continuous wave signal with an output power of +17.6 dBm at 5.8 GHz. It is worth remarking that the TX was pre-calibrated using a Rhode & Schwarz NRP-Z21 power meter. The RX also featured an ML5805 transceiver attached to a PIC32MX microcontroller which acted as a baseband controller programmed to sample the analog RSS at a rate of 10 kHz from the ML5805 transceiver using a 10-bit analog-to-digital converter (ADC). All of the RXs were pre-calibrated using a Rohde & Schwarz SMU200A vector signal generator. For both the TX and RX, a +2.3 dBi sleeve dipole antenna (Mobile Mark PSKN3-24/55S)³ was connected directly to the RF front end of the radio using a SubMiniature version A connector.

The TX was mounted vertically on the front-central chest region of an adult male of mass 75 kg and height 1.72 m using Velcro so that the antenna was parallel to the pedestrian's body. To maintain a consistent antenna-body separation distance throughout the measurements, a 5 mm dielectric spacer consisting of Rohacell HF 51 foam was placed between the antenna and the body surface. As shown in Fig. 1, the hypothetical DAS antennas were positioned at six different locations of the vehicle exterior. These are front-center of the roof (Ant. 1), left-wing mirror (Ant. 2), right-wing mirror (Ant. 3), rear-center of the roof (Ant. 4), rear-left of the roof (Ant. 5) and rear-right of the roof (Ant. 6). It should be noted that all the DAS antennas were mounted in a vertically polarized orientation. The roof-mounted antennas were secured directly onto the vehicle's body. However, due to the physical dimensions of the antennas, the base of the antenna maintained a distance of 30 mm from the roof surface. To emulate the placement of the antenna inside the wing mirror unit, the antenna was mounted on the outside edge of the wing mirror with the same type of dielectric spacer as used on the pedestrian's body. These on-vehicle locations were chosen as candidate antenna mounting positions for DASs used in future vehicular applications. The vehicle used for the measurements was a typical European, small three-door hatchback car with the dimensions as depicted in Fig. 1. Further details on the antennas used for the TX and RX are available in [12] including a visual illustration of the mounting arrangement and measured azimuthal antenna radiation patterns for the

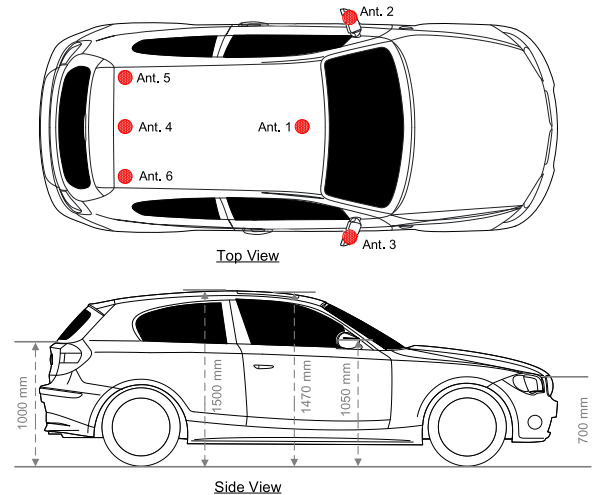


Fig. 1. Antenna locations on the vehicle and their heights relative to the road.

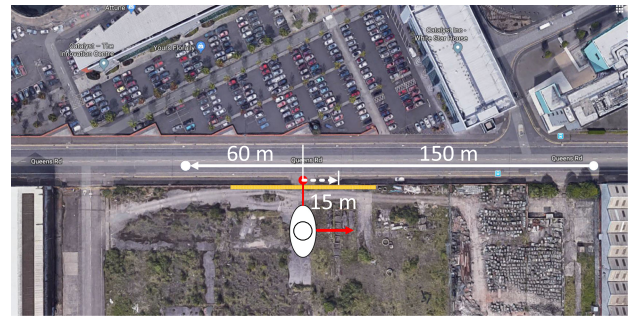


Fig. 2. P2V channel measurement location along with the vehicle trajectories (white continuous lines with an arrowhead) and pedestrian trajectory (white dashed lines with an arrowhead) for the walking scenarios. It is worth noting that the red arrow indicates the direction that the pedestrian was facing (note: Image courtesy of Google Maps).

TX mounted on user's / test subject's body and for the RX mounted on the vehicle's roof and wing mirrors.

B. Measurement Environment and Scenarios

All of the P2V channel measurements were performed on a straight stretch of road situated within a business district in the Titanic Quarter of Belfast, United Kingdom (U.K.) as shown in Fig. 2. The surrounding area contained a number of large office buildings situated at various distances and orientations relative to the roadside. The vehicle's trajectory was limited to the straight stretch of road, however, as is typical with urban environments other vehicles may travel along the near side or the far side of the road relative to the pedestrian. The road is approximately 10 m in width and there exists a wall approximately 2 m in height that ran along the sidewalk near the pedestrian (see the yellow continuous line in Fig. 2). For the P2V channel measurements, we considered two different movement scenarios for the pedestrian, namely stationary and walking. In the stationary scenario, the pedestrian stood static and parallel to the roadside, while oriented toward the direction of the oncoming vehicle. In the walking scenario, the pedestrian walked parallel to the roadside, again oriented toward the direction of the oncoming vehicle. For both the stationary and walking scenarios, the vehicle traveled on the side of the road closest to the pedestrian. During the measurements, the pedestrian walked with a velocity of approximately 1.2 m/s, covering a

²<http://datasheet.octopart.com/ML5805DM-Micro-Linear-datasheet-8614608.pdf> (visited on 03/26/2021).

³<https://mobilemark.com/product/pskn3-24-55/> (visited on 03/26/2021).

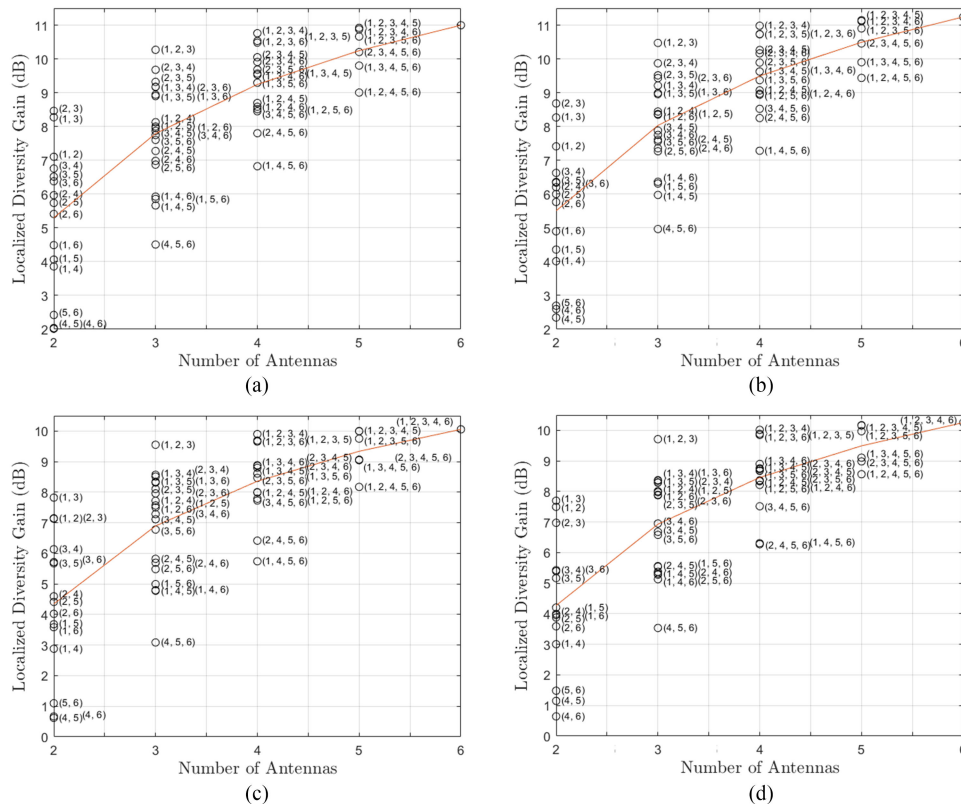


Fig. 3. Mean localized diversity gains averaged over all time slots for the different number of antennas with all possible groupings of antennas: (a) stationary with short-term case; (b) stationary with long-term case; (c) walking with short-term case; (d) walking with long-term case.

distance of 15 m (as indicated by white dashed lines with an arrowhead in Fig. 2). In accordance with U.K. traffic laws for a single carriageway road, in both the stationary and walking scenarios, the vehicle maintained a velocity of 13.4 m/s (or equivalently 30 mph) while traveling in the left hand lane.

III. LOCALIZED DIVERSITY GAIN

Prior to the data analysis and using the approach described in [28], the received signal power was transformed into the received signal-to-noise ratio (SNR). The potential improvement in the received signal reliability that could be achieved using the SECps based DAS system was evaluated using the measured diversity gain. We define the diversity gain as the improvement in the received SNR at the output of the DAS compared to the received SNR at the target antenna for a given signal reliability. For the purposes of the investigation performed here, Ant. 1 was considered as the target antenna and all diversity gain calculations were made at the signal reliability of 90%. In this study, we consider the concept of *localized diversity gain* introduced in [29], [30]. This can be obtained by considering a moving window of length N applied to the recorded data. Within each window, we combined the raw RSS from the relevant antennas on a sample by sample basis using the SECps scheme. For each realization of the moving window, we then calculated the diversity gain as described above. This process was repeated as the window of length N was moved across the recorded data to obtain the localized diversity gain time series. Unlike the global diversity gain⁴, the localized diversity gain as calculated here is a time series, which enables us to fully capture the temporal behavior of the diversity gain. Two different values of N were considered in this study to

TABLE I
AVERAGE SNR (IN DECIBELS) AT EACH ANTENNA

	Ant. 1	Ant. 2	Ant. 3	Ant. 4	Ant. 5	Ant. 6
Stationary	33.2	35.5	34.9	29.1	29.3	29.3
Walking	35.5	37.2	36.1	30.3	30.9	30.8

investigate the impact of different window sizes on the localized diversity gain. These values are 2,000 and 20,000 which are equivalent to 0.2 (short-term) and 2 (long-term) seconds, respectively.⁵

Fig. 3 shows the mean localized diversity gain averaged over all time slots for the different number of the antennas with all possible groupings of the antennas.⁶ The mean diversity gain averaged over all possible groupings of the antennas for the different number of antennas is also presented in Fig. 3 (see the red continuous lines). For both the short- and long-term cases, the mean localized diversity gain for the stationary scenario was found to be higher than that for the walking

⁴The entire data set recorded at each antenna is taken into account to obtain the global diversity gain, i.e., only one value for each scenario. Therefore, the global diversity gain is not able to capture the temporal behavior of the diversity gain.

⁵The vehicle travels 2.68 m and 26.8 m for 0.2 and 2 seconds, respectively. These travel distances are equivalent to approximately 50λ and 500λ with λ denoting the wavelength and therefore they are denoted as ‘short-term’ and ‘long-term’ in this study, respectively.

⁶The total number of all possible grouping of the antennas are 15, 20, 15, 6 and 1 for $L = 2, 3, 4, 5$ and 6, respectively (see Fig. 3).

TABLE II
PARAMETER ESTIMATES FOR THE GAUSSIAN DISTRIBUTION FOR ALL OF THE CONSIDERED SCENARIOS ALONG WITH THE RAD

Number of antennas (L)	Stationary						Walking					
	short-term			long-term			short-term			long-term		
	μ	σ	RAD	μ	σ	RAD	μ	σ	RAD	μ	σ	RAD
2	5.3	5.5	0.0065	5.5	3.7	0.0087	4.3	6.8	0.0177	4.3	4.4	0.0077
3	7.8	5.2	0.0059	8.0	3.5	0.0117	6.9	6.5	0.0161	6.9	4.3	0.0069
4	9.2	5.1	0.0060	9.5	3.4	0.0151	8.4	6.3	0.0152	8.5	4.3	0.0084
5	10.2	5.1	0.0062	10.5	3.4	0.0189	9.3	6.3	0.0145	9.5	4.3	0.0127
6	11.0	5.1	0.0067	11.2	3.4	0.0237	10.1	6.3	0.0142	10.3	4.4	0.0206

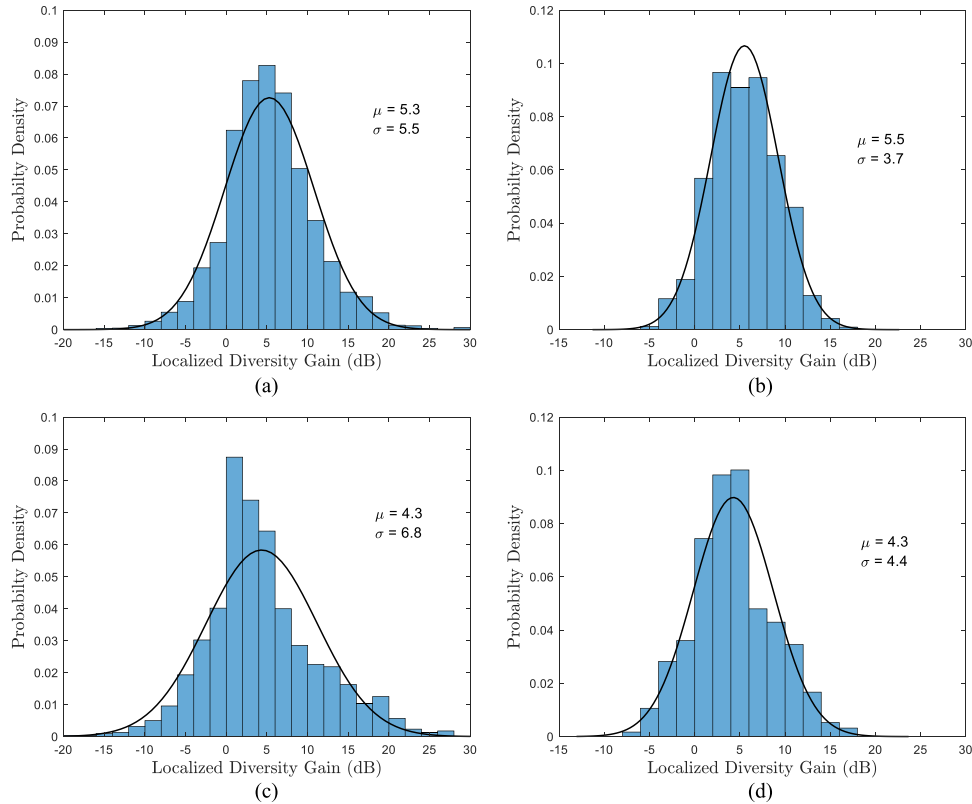


Fig. 4. Empirical PDFs of the localized diversity gain along with the corresponding Gaussian PDF fits when $L = 2$: (a) stationary with short-term case, (b) stationary with long-term case, (c) walking with short-term case, and (d) walking with long-term case.

scenario. As shown in Table I, due to the additional multipath for the walking scenario which may have helped to mitigate the shadowing caused by the pedestrian's body and/or vehicle's body, the average SNR of all antennas for the walking scenario was greater than that for the stationary scenario. In particular, the average SNR at Ant. 1 (the target antenna) increased from 33.2 dB to 35.5 dB when the pedestrian walked. This increment (2.3 dB) was greater than those for Ants. 2-6 (which ranged from 1.2 dB to 1.7 dB). Consequently, for this configuration, the diversity gain for the walking scenario was smaller compared to the stationary scenario. However, the diversity gain was dependent on the choice of the target antenna. For example, when Ant. 2 or Ant. 3 was selected as the target antenna, the diversity gain for the walking scenario was observed to be greater than that for the stationary one. Since the average SNR at Ants. 4-6 are lower than those at Ants. 1-3 (Table I), the mean localized diversity gain achieved by the majority of groupings with Ants. 4-6 are below the red lines (i.e., lower than the average) for all of the considered cases. Moreover, for both the stationary and walking scenarios, there exists no significant difference

in the mean localized diversity gain between short- and long-term cases.

To facilitate a further investigation of the statistics of the localized diversity gain, the parameter estimates for a Gaussian distribution, i.e., mean (μ) and standard deviation (σ), are presented in Table II. For all of the considered cases, the μ values presented in Table II are in good agreement with the mean localized diversity gain averaged over all possible groupings of the antennas presented as red continuous lines in Fig. 3. Consulting the σ values presented in Table II, for both the short- and long-term cases, the σ values for the walking scenario were observed to be greater than those for the stationary scenario. This may be attributed to the fact that as the pedestrian walked, the link between the pedestrian and vehicle for the walking scenario became more susceptible to signal fluctuations compared to that for the stationary scenario. This was a direct result of the joint mobility of the pedestrian and the vehicle. For both the stationary and walking scenarios, the σ values for the short-term case were observed to be greater than those for the long-term case.

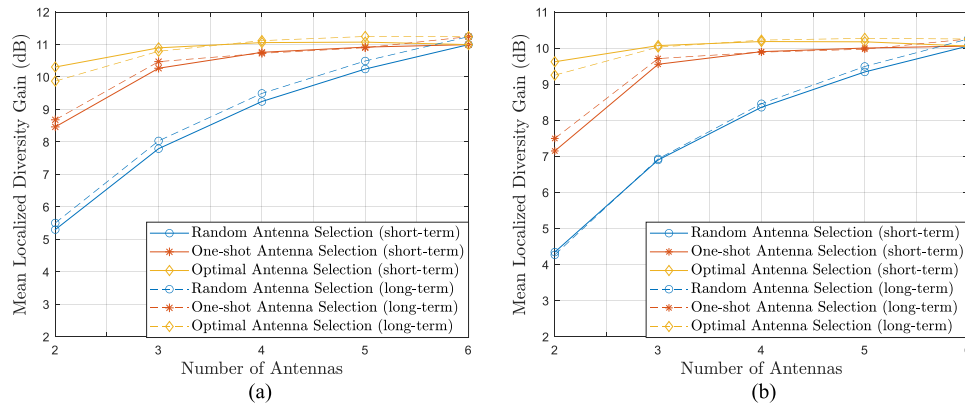


Fig. 5. Mean localized diversity gain vs number of antennas for the different antenna selection schemes: (a) stationary; and (b) walking scenarios.

As an example of the model fitting, Fig. 4 shows the empirical probability density functions (PDFs) of the short- and long-term localized diversity gain for the stationary scenario ($L = 2$) alongside the Gaussian PDF fits. It is apparent that the Gaussian distribution provided an adequate fit to the empirical data. This is supported by the resistor-average distance (RAD) which was used as a quantitative measure of the goodness-of-fit of a Gaussian distribution with the empirical data. The RAD is a symmetric version of the Kullback-Leibler divergence and thus satisfies the triangle inequality, representing a true distance metric [31]. As shown in Table II, the minimum and maximum RAD values were found to be 0.0059 and 0.0237 respectively, suggesting that the Gaussian distribution generally provided a satisfactory fit to the measured data. Additionally, it was apparent that the Gaussian distribution provided a better fit for the short-term localized diversity gain compared to the long-term case. This was most likely due to the chosen window size. More specifically, as N increases, the number of wavelengths (i.e., distance) contained within the moving window also increases, which can yield a significant change in the characteristics of the signal propagation.

IV. ANTENNA SELECTION MECHANISMS

In the previous section, it has been demonstrated that the SECps based DASs provided considerable improvement in the overall signal reliability. However, their performance varied according to not only the number of the antennas but also the grouping of antennas which were selected. To further investigate their influence on the performance, in this section, we compute the mean localized diversity gain using the different antenna selection mechanisms presented in [26], [27], namely per-sample random antenna selection, one-shot antenna selection and per-sample optimal antenna selection. In per-sample random antenna selection, the grouping of the antennas is determined from the set of candidate antennas (i.e., six antennas in this study) at each sample interval [26]. Since antennas are selected randomly, there is no need to measure and compare the diversity gain achieved by each grouping. Notably this approach achieves low implementation complexity. On the other hand, at every single time slot, per-sample optimal antenna selection examines the diversity gain for each grouping and finds the optimal grouping of the antennas. Clearly, this approach offers the best performance, but it is also the most complicated [27]. Therefore, for both the random and optimal antenna selection schemes, it is possible that a different grouping of the antennas can be selected at every single sample interval. Unlike these two schemes, under the one-shot antenna selection scheme [27], the connections between the pedestrian and vehicle established in the first time slot are maintained, i.e., there

are no changes beyond the first time slot. As a result, the wireless node positioned on the pedestrian simply selects the grouping of the antennas which has the highest diversity gain and persists with this configuration. It is worth highlighting that the SECps scheme is still employed to choose one antenna from the grouping of the antennas determined at each sample interval for all of three antenna selection mechanisms.

Fig. 5 shows the effect of different antenna selection schemes on the diversity performance. As expected, the random antenna selection scheme offers the worst performance, while the optimal antenna selection scheme performs best. For example, when $L = 3$ and considering the stationary scenario with a short-term window, the corresponding mean localized diversity gain for the random and optimal antenna selection schemes are 7.8 dB and 10.9 dB respectively. Additionally, the optimal antenna selection scheme with $L = 2$ can achieve almost the same performance as the random antenna selection scheme with $L = 5$. As the number of the antennas increases, the diversity gain obtained for the random antenna selection scheme significantly increases (almost linearly). In contrast, for the one-shot and optimal antenna selection schemes, the achievable diversity gain became saturated beyond a certain number of the antennas, i.e., $L = 4$ and $L = 3$ for the one-shot and optimal antenna selection schemes, respectively.

V. CONCLUSION

The potential improvement in the received signal reliability for P2V communications at 5.8 GHz using a SECps based DAS has been evaluated in terms of the localized diversity gain. Although the magnitude of the localized diversity gain depended on how many antennas were selected and how they were grouped, overall the SECps based DAS provided a worthwhile signal improvement and will have merit when used for pedestrian safety-related applications. The temporal behavior of the diversity gain was modeled using a Gaussian distribution, whose characteristics varied according to the pedestrian's movement and chosen window size. Additionally, based on our analysis, it was found that the optimal antenna selection scheme provided the best performance, followed by the one-shot and random antenna selection schemes. Unlike the random antenna selection scheme, the achievable diversity gain obtained by adding antennas for the one-shot and optimal antenna selection schemes was found to saturate as the number of the antennas increased. When considering this saturation and the additional complexity introduced by including more antennas in the DAS, the optimum number of the antennas was determined as $L = 4$ and $L = 3$ for the one-shot and optimal antenna selection schemes, respectively.

REFERENCES

- [1] X. Wang, S. Mao, and M. X. Gong, "An overview of 3GPP cellular vehicle-to-everything standards," *GetMobile: Mobile Comput. Commun.*, vol. 21, no. 3, pp. 19–25, Sep. 2017.
- [2] P. Merdrignac, O. Shagdar, and F. Nashashibi, "Fusion of perception and V2P communication systems for the safety of vulnerable road users," *IEEE Trans. Intell. Transp. Syst.*, vol. 18, no. 7, pp. 1740–1751, Jul. 2017.
- [3] X. Wu *et al.*, "Cars talk to phones: A DSRC based vehicle-pedestrian safety system," in *Proc. IEEE 80th Veh. Technol. Conf.*, Sep. 2014, pp. 1–7.
- [4] M. Boban, R. Meireles, J. Barros, P. Steenkiste, and O. K. Tonguz, "TVR-tall vehicle relaying in vehicular networks," *IEEE Trans. Mobile Comput.*, vol. 13, no. 5, pp. 1118–1131, May 2014.
- [5] A. A. M. Saleh, A. J. Rustako, and R. Roman, "Distributed antennas for indoor radio communications," *IEEE Trans. Commun.*, vol. 35, no. 12, pp. 1245–1251, Dec. 1987.
- [6] S. Kaul *et al.*, "Effect of antenna placement and diversity on vehicular network communications," in *Proc. 4th Annu. IEEE Commun. Soc. Conf. Sensor, Mesh Ad Hoc Commun. Netw.*, Jun. 2007, pp. 112–121.
- [7] M. D. Yacoub, *Foundations of Mobile Radio Engineering*. Boca Raton, FL, USA: Routledge, 2019.
- [8] C.-S. Kim, H.-J. Kim, J.-S. Lim, J.-Y. Hong, and Y. Chong, "Measurement results of high-speed V2X channel characteristics in expressway environment," in *Proc. Int. Symp. Antennas Propag.*, Oct. 2018, pp. 1–2.
- [9] M. N. Sial, Y. Deng, J. Ahmed, A. Nallanathan, and M. Dohler, "Stochastic geometry modeling of cellular V2X communication over shared channels," *IEEE Trans. Veh. Technol.*, vol. 68, no. 12, pp. 11 873–11 887, Oct. 2019.
- [10] C. Gustafson, K. Mahler, D. Bolin, and F. Tufvesson, "The cost iracon geometry-based stochastic channel model for vehicle-to-vehicle communication in intersections," *IEEE Trans. Veh. Technol.*, vol. 69, no. 3, pp. 2365–2375, Jan. 2020.
- [11] I. Rashdan, F. D. P. Müller, T. Jost, S. Sand, and G. Caire, "Large-scale fading characteristics and models for vehicle-to-pedestrian channel at 5 GHz," *IEEE Access*, vol. 7, pp. 107 648–107 658, Aug. 2019.
- [12] M. G. Doone, S. L. Cotton, D. W. Matolak, C. Oestges, S. F. Heaney, and W. G. Scanlon, "Pedestrian-to-vehicle communications in an urban environment: Channel measurements and modeling," *IEEE Trans. Antennas Propag.*, vol. 67, no. 3, pp. 1790–1803, Mar. 2019.
- [13] G. Makhoul, R. D'Errico, and C. Oestges, "Wideband vehicle to pedestrian propagation channel characterization and modeling," in *Proc. 12th Eur. Conf. Antennas Propag.*, Apr. 2018, pp. 1–4.
- [14] K. Maliatsos, L. Marantis, P. S. Bithas, and A. G. Kanatas, "Hybrid multi-antenna techniques for V2X communications-prototyping and experimentation," *Telecom*, vol. 1, no. 2, pp. 80–95, Jul. 2020.
- [15] M. M. Ginard, T. Izydorczyk, P. Mogensen, and G. Berardinelli, "Enhancing vehicular link performance using directional antennas at the terminal," in *Proc. IEEE Globecom Workshops*, Dec. 2019, pp. 1–5.
- [16] M. Yusuf *et al.*, "Experimental study on the impact of antenna characteristics on non-stationary V2I channel parameters in tunnels," *IEEE Trans. Veh. Technol.*, vol. 69, no. 11, pp. 12 396–12 407, Aug. 2020.
- [17] Y. Alghorani and M. Seyfi, "On the performance of reduced-complexity transmit/receive-diversity systems over MIMO-V2V channel model," *IEEE Wireless Commun. Lett.*, vol. 6, no. 2, pp. 214–217, Jan. 2017.
- [18] T. Abbas, J. Karedal, and F. Tufvesson, "Measurement-based analysis: The effect of complementary antennas and diversity on vehicle-to-vehicle communication," *IEEE Antennas Wireless Propag. Lett.*, vol. 12, pp. 309–312, Mar. 2013.
- [19] F. Jameel, M. A. Javed, and D. T. Ngo, "Performance analysis of cooperative V2V and V2I communications under correlated fading," *IEEE Trans. Intell. Transp. Syst.*, vol. 21, no. 8, pp. 3476–3484, Jul. 2019.
- [20] C. Stefanovic, S. Veljkovic, M. Stefanovic, S. Panic, and S. Jovkovic, "Second order statistics of sir based macro diversity system for V2I communications over composite fading channels," in *Proc. 1st Int. Conf. Secure Cyber Comput. Commun.*, Dec. 2018, pp. 569–573.
- [21] A. P. Sohrab, P. Karadimas, and Y. Huang, "Diversity antenna for vehicular communications in microwave and mm-wave bands," in *Proc. IEEE-APS Topical Conf. Antennas Propag. Wireless Commun.*, Sep. 2019, pp. 109–111.
- [22] J. B. Kenney, "Dedicated short-range communications (DSRC) standards in the United States," *Proc. IEEE*, vol. 99, no. 7, pp. 1162–1182, Jul. 2011.
- [23] S. K. Yoo, S. L. Cotton, and W. G. Scanlon, "Switched diversity techniques for indoor off-body communication channels: An experimental analysis and modeling," *IEEE Trans. Antennas Propag.*, vol. 64, no. 7, pp. 3201–3206, Jul. 2016.
- [24] H. C. Yang and M.-S. Alouini, "Performance analysis of multibranch switched diversity systems," *IEEE Trans. Commun.*, vol. 51, no. 5, pp. 782–794, May 2003.
- [25] S. K. Yoo, L. Zhang, S. L. Cotton, and H. Q. Ngo, "Distributed antenna systems used for indoor UE to access point communications at 60 GHz," in *Proc. 13th Eur. Conf. Antennas Propag.*, Apr. 2019, pp. 1–5.
- [26] C. Skouroumounis, C. Psomas, and I. Krikidis, "Low-complexity base station selection scheme in mmWave cellular networks," *IEEE Trans. Commun.*, vol. 65, no. 9, pp. 4049–4064, Sep. 2017.
- [27] X. Qin, X. Yuan, Z. Zhang, F. Tian, Y. T. Hou, and W. Lou, "Joint user-AP association and resource allocation in multi-AP 60-GHz WLAN," *IEEE Trans. Veh. Technol.*, vol. 68, no. 6, pp. 5696–5710, Jun. 2019.
- [28] S. K. Yoo, S. L. Cotton, W. G. Scanlon, and G. Conway, "An experimental evaluation of switched combining based macro-diversity for wearable communications operating in an outdoor environment," *IEEE Trans. Wireless Commun.*, vol. 16, no. 8, pp. 5338–5352, Aug. 2017.
- [29] L. J. November, "Measurement of geometric distortion in a turbulent atmosphere," *Appl. Opt.*, vol. 25, no. 3, pp. 392–397, Feb. 1986.
- [30] L. Zhang *et al.*, "A time series based study of correlation, channel power imbalance and diversity gain in indoor distributed antenna systems at 60 GHz," *IEEE Trans. Antennas Propag.*, to be published, doi: 10.1109/TAP.2021.3076171.
- [31] D. H. Johnson and S. Sinanovic, *Symmetrizing the Kullback-Leibler Distance*. Houston Rice Univ. Working Paper, 2001.